歩行者高さにおける低頻度で発生する高風速のワイブル分布に基づく統計的予測
Statistical methods for estimating low-occurrence strong wind speeds at the pedestrian level based on the Weibull distribution

王偉[*1, 2]，大風翼[*2]，池谷直樹[*1]
Wei WANG, Tsubasa OKAZE, Naoki IKEGAYA

The low-occurrence strong wind speed (LOSWS) at the pedestrian level is important regarding the human and structure safety. Although several statistical methods were developed in previous studies, their accuracy and applicability for the cases with various building layouts remain unclear. This study analyzed the performances of two statistical methods (3W and 2W methods) for estimating the LOSWS at the pedestrian level of an isolated building case (Case-IB) and an actual urban case (Case-TPU). The 3W and 2W methods are based on the three-parameter and two-parameter Weibull distributions, respectively. The LES result of Case-IB was from a validated LES database. The LES of Case-TPU was validated with a wind tunnel experiment, and was found to have acceptable accuracy. It was found that the peak factors with exceedance probabilities q = 10%, 1% and 0.1% of the 3W and 2W methods are close to those of the LES results. The relative errors of the LOSWSs with q = 10%, 1% and 0.1% predicted by both methods are within 10% at most probe points for both cases. The high accuracy and robustness of the 3W and 2W methods were confirmed. The findings in this study are supportive to the further applications of these statistical methods in urban area cases.

1. Introduction

With the advancement of urbanization, increasing numbers of buildings have been built in recent decades. Changes in the landscape have significantly affected wind patterns in urban areas. Flow separations, downwashes, and vortex shedding around buildings are combined (Cao et al., 2019; Wang et al., 2006), making the pedestrian-level wind environment (PLWE) highly complex in urban areas (Stathopoulos, 2006). To reduce the risk caused by strong winds, low-occurrence strong wind speeds (LOSWSs) at the pedestrian level have received significant attention. Most wind environment criteria from different countries and regions (Isyumov and Davenport, 1975; Murakami et al., 1986; Soligo et al., 1998) have been proposed based on a combination of threshold wind speeds and the probabilities of exceeding the corresponding thresholds.

Recently, several researchers have conducted large-eddy simulations (LESs) to accurately evaluate LOSWSs at the pedestrian level (Ikegaya et al., 2020, 2017; Kawaminami et al., 2018). However, the cost of such high-fidelity techniques, which can directly provide the wind speed or velocity components at each percentile, is significantly high (Blocken et al., 2016; Vita et al., 2020). Consequently, the studies on LOSWSs are limited.

An alternative way to estimate LOSWSs is to use statistical methods with statistics. However, only a few statistical methods (Efthimiou et al., 2017; Wang and Okaze, 2022), which relate statistics to LOSWSs, are available because of the complex nature of turbulence. Wang and Okaze, 2022 developed two statistical methods based on the two-parameter and three-parameter Weibull distributions (i.e., 2W and 3W) for estimating LOSWSs using statistics. The 2W method requires the mean and standard deviation of wind speed

*1 九州大学総合理工学研究院　wang.wei.530@m.kyushu-u.ac.jp
Faculty of Engineering Sciences, Kyushu University
*2 東京工業大学環境・社会理工学院
School of Environment and Society, Tokyo Institute of Technology

and the 3W method requires the mean, standard deviation and skewness of wind speed. Although the 2W and 3W methods were already validated to have high accuracy for an isolated building case, their performances for actual urban cases still remain unclear. Consequently, this study aims to validate the accuracy and robustness of the 2W and 3W methods for an actual urban case. The results of the isolated building case were also presented as a reference.

2. Weibull distribution

The cumulative distribution function $F(x)$ and probability density function $f(x)$ of 3W are defined in Eqs. (1) and (2), respectively (Weibull, 1951). $\alpha > 0$ is the scale parameter, $\beta > 0$ is the shape parameter, and ζ is the location parameter. 2W is a special case of 3W when the location parameter $\zeta = 0$.

The mean μ, standard deviation σ, and skewness γ of 3W can be mathematically expressed by Eqs. (3)–(5), respectively. The detailed derivations can be found in Rinne, 2008. For 2W, the coefficient of variation (CV) is expressed as Eq. (6). The value of x_q with exceedance probability q for 3W can be derived from Eq. (1) as Eq. (7). The peak factor (PF) K_q with exceedance probability q for 3W can be derived from Eqs. (3), (4), (7) as Eq. (8) (Wang and Okaze, 2022). Note that the PFs of 2W and 3W are the same to each other.

$$F(x) = 1 - \exp\left[-\left(\frac{x-\zeta}{\alpha}\right)^{\beta}\right] \quad , \ x \geq \zeta \tag{1}$$

$$f(x) = \frac{\beta}{\alpha}\left(\frac{x-\zeta}{\alpha}\right)^{\beta-1} \exp\left[-\left(\frac{x-\zeta}{\alpha}\right)^{\beta}\right] \quad , \ x \geq \zeta \tag{2}$$

$$\mu = \zeta + \alpha\Gamma(1 + 1/\beta) \tag{3}$$

$$\sigma = \alpha[\Gamma(1 + 2/\beta) - \Gamma^2(1 + 1/\beta)]^{1/2} \tag{4}$$

$$\gamma = \frac{\Gamma(1 + 3/\beta) - 3\Gamma(1 + 2/\beta)\Gamma(1 + 1/\beta) + 2\Gamma^3(1 + 1/\beta)}{[\Gamma(1 + 2/\beta) - \Gamma^2(1 + 1/\beta)]^{3/2}} \tag{5}$$

$$\sigma/\mu = \frac{[\Gamma(1 + 2/\beta) - \Gamma^2(1 + 1/\beta)]^{1/2}}{\Gamma(1 + 1/\beta)} \quad , \text{for 2W} \tag{6}$$

$$x_q = \zeta + \alpha[-\ln(q)]^{1/\beta} \tag{7}$$

$$K_q = \frac{x_q - \mu}{\sigma} = \frac{[-\ln(q)]^{1/\beta} - \Gamma(1 + 1/\beta)}{[\Gamma(1 + 2/\beta) - \Gamma^2(1 + 1/\beta)]^{1/2}} \tag{8}$$

$$\langle s \rangle_{\text{Eff}} = (\langle u \rangle^2 + \langle v \rangle^2 + \langle w \rangle^2 + 2k)^{1/2} \tag{9}$$

$$s_q = \mu + K_q\sigma \tag{10}$$

3. Numerical settings of LES

3.1. Isolated building case

The wind field around a 1:1:2 isolated building (Case-IB) predicted by the LES in the authors' previous studies (Ikegaya et al., 2019; Okaze et al., 2021, 2017; Wang et al., 2021) was used as the wind speed database in this study. The details of the LES settings can be found in Okaze et al., 2021, 2017 as "Case-2-linear0.95". The LES results were validated through a wind tunnel experiment (WTE) conducted at Tokyo Polytechnic University as the benchmark Case-H provided by the AIJ ("AIJ benchmark Case-H"). The computational domain is illustrated in Fig. 1 (a). The height and width of the building are H = 0.2 m and B = 0.1 m, respectively. The origin of the coordinate system is the midpoint of the intersection between the leeward wall of the building and ground. The distribution of the probe points (80 points in total) at the pedestrian level of Case-IB is shown in Fig. 1 (b).

3.2. Actual urban case

The computational domain of the Tokyo Polytechnic University Atsugi Campus (Kanagawa, Japan) case

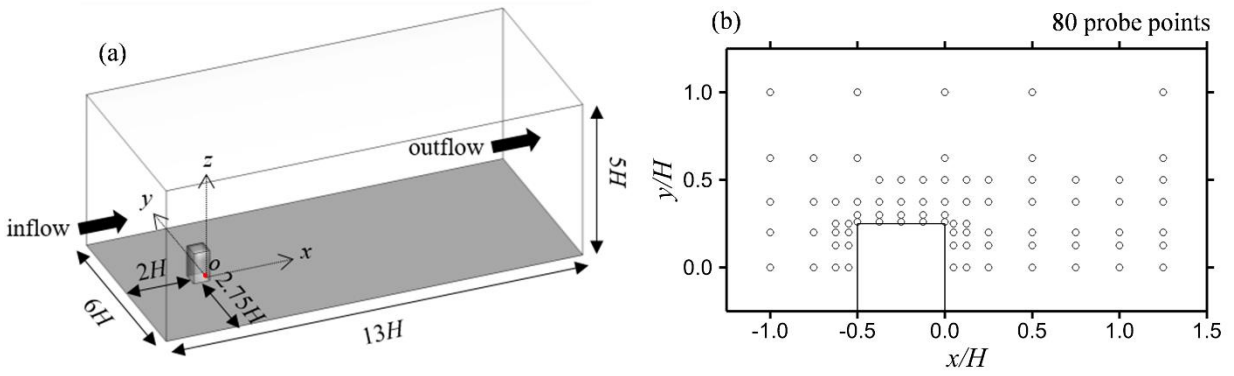

Fig. 1. Case-IB. (a) Computational domain (H denotes the height of the building; o denotes the origin of the coordinate system); (b) distribution of the probe points at the pedestrian level to record the time-series data.

(Case-TPU) is shown in Fig. 2. The building geometry was constructed by using AW3D building data (https://www.aw3d.jp/en/products/building/). The scale ratio between the model scale and full scale was 1/600. The buildings with the green color are the buildings of the university, while the buildings with the dark grey color are the surrounding buildings. The computational domain size was consistent with that of the WTE (Tachibana et al., 2017). Fig. 2 (b) shows a top view of the computational domain. The approaching length from the inlet boundary to the buildings was larger than $5H_{max}$, where H_{max} is the maximum building height of Case-TPU. The wake region from the interested area (highlighted by the red lines in Fig. 2 (b)) to the outlet boundary was larger than $15H_{max}$. The side boundaries were set approximately 6–10 H_{near} away from the buildings, where H_{near} is the height of the buildings near the side boundaries. The distances between buildings and boundaries fulfilled the requirements of the AIJ guideline (Tominaga et al., 2008). The distribution of the probe points (20 points in total) to record the time-series data is shown in Fig. 3.

4. Validation of Case-TPU

The comparisons of the effective mean wind speed (defined in Eq. (9)) and standard deviation of the streamwise velocity between the WTE (Tachibana et al., 2017) and LES are shown in Fig. 4. It was found that the effective mean wind speed of the LES was close to that of the WTE (i.e., differences were within

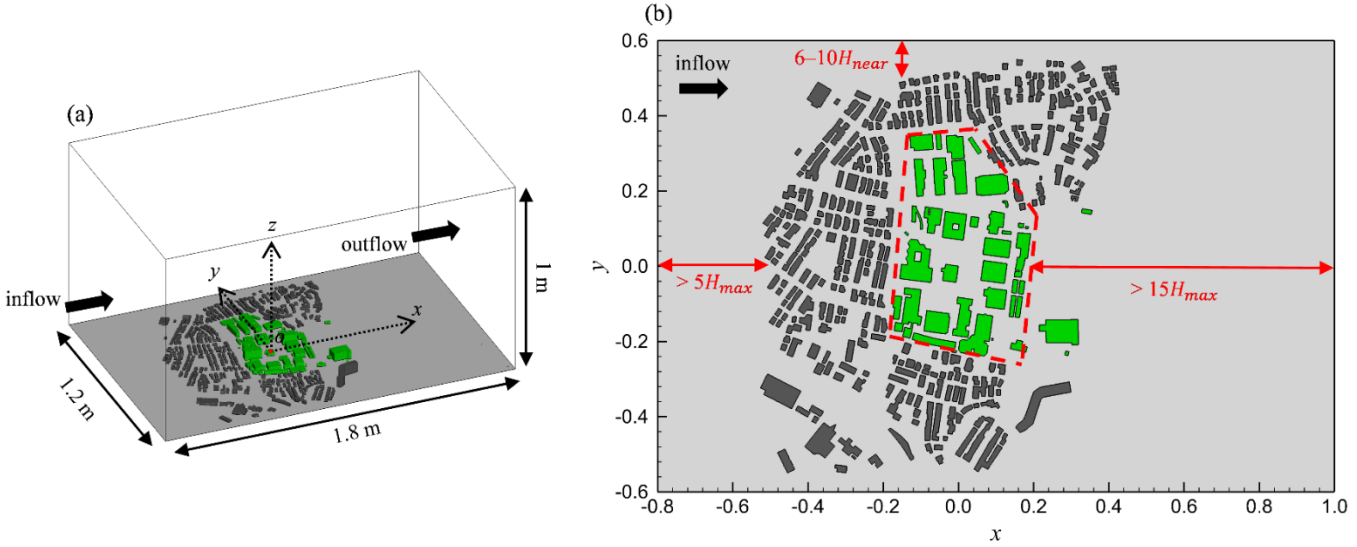

Fig. 2. Computational domain of Case-TPU. (a) Three-dimensional view; (b) top view. The green color denotes the buildings inside the campus. The dark grey color denotes the surrounding buildings. The highlighted region in (b) is of interest in this study. H_{max} is the maximum building height of Case-TPU. H_{near} is the height of the building near side boundaries.

Fig. 3. Building layout and probe point distribution. The scale ratio between the model scale (WTE and LES) and full scale is 1/600. The red circles are the probe points in the WTE. The black circles are the additional probe points in this study. Totally, 20 probe points were distributed at the pedestrian level (2 m) in the LES. The blue cross denotes the reference point, which is located at Z_r = 41 m above the ground in the full scale.

approximately ±20% at most points) as shown in Fig. 4 (a). At P7 (see Fig. 3), the LES result has a relatively large difference with the WTE result for the effective mean wind speed, which is caused by the absence of the building beside P7 as shown in Fig. 3 (the geometric model in the WTE was not updated while that in the LES is the newest building layout). Moreover, P14 and P15 are located in the leeward side of mountains in the WTE, but the effects of topology were neglected in the LES for the simplification; consequently, the effective mean wind speeds of the LES at P14 and P15 have relatively large differences with those of the WTE. In Fig. 4 (b), although the standard deviations from the LES have some differences with those from the WTE, the values were still comparable to each other at most points. In previous studies of the PLWE in actual urban areas (Hertwig et al., 2017; Vita et al., 2020), comparable discrepancies between LESs and WTEs as those in this study were observed because the complicated building layouts bring relatively large uncertainty in both simulations and experiments. Overall, although the geometric shapes of the buildings in Case-TPU are significantly complex, the accuracy of the LES is acceptable.

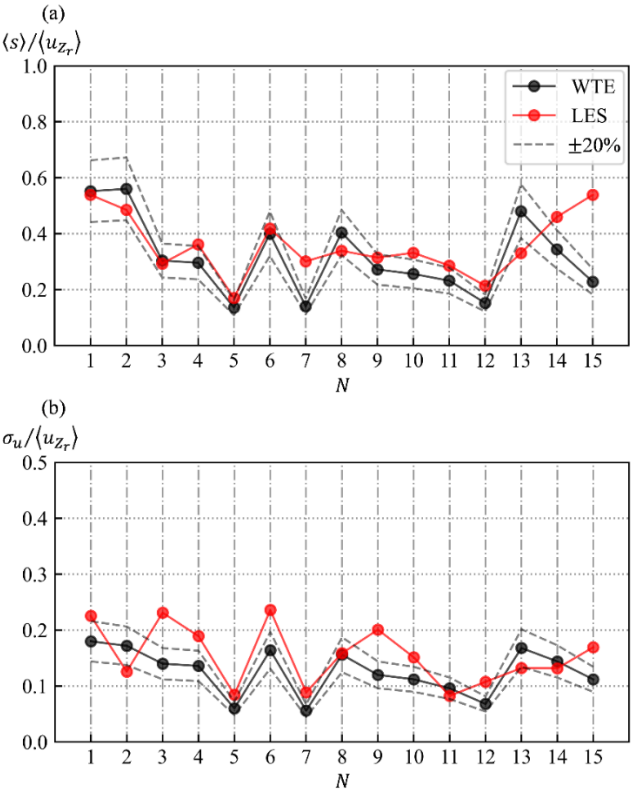

Fig. 4. Comparison of statistics between the WTE and LES. (a) Effective mean wind speed; (b) standard deviation of the streamwise velocity. The dashed line denotes the ±20% deviations of the WTE. It should be mentioned that the horizontal locations of point-1–point-15 are the same as those in Fig. 3, but the height of the points in this figure are 3 m in the full scale, because the WTE (Tachibana et al., 2017) only provided the data at the 3 m height.

5. Estimation of LOSWS

Fig. 5 (a, b) show the comparison of statistics with PFs for q = 10%, 1% and 0.1% of Case-IB. The x-axis in Fig. 5 (a) denotes the skewness γ and in Fig. 5 (b) denotes the CV σ/μ. The y-axis denotes the PF. The curves are the theoretical relationships of 3W (Fig. 5 (a, c)) or 2W (Fig. 5 (b, d)) (Wang and Okaze, 2022). The scatters are the LES results. It is clear that 3W well predicted the PFs for q = 10% and 1%. For q = 0.1%, although the deviations between the LES and 3W are larger than those for q = 10% and 1%, the increasing trend between γ and K_q of the LES still can be captured by the curve of 3W. In Fig. 5 (b), for larger

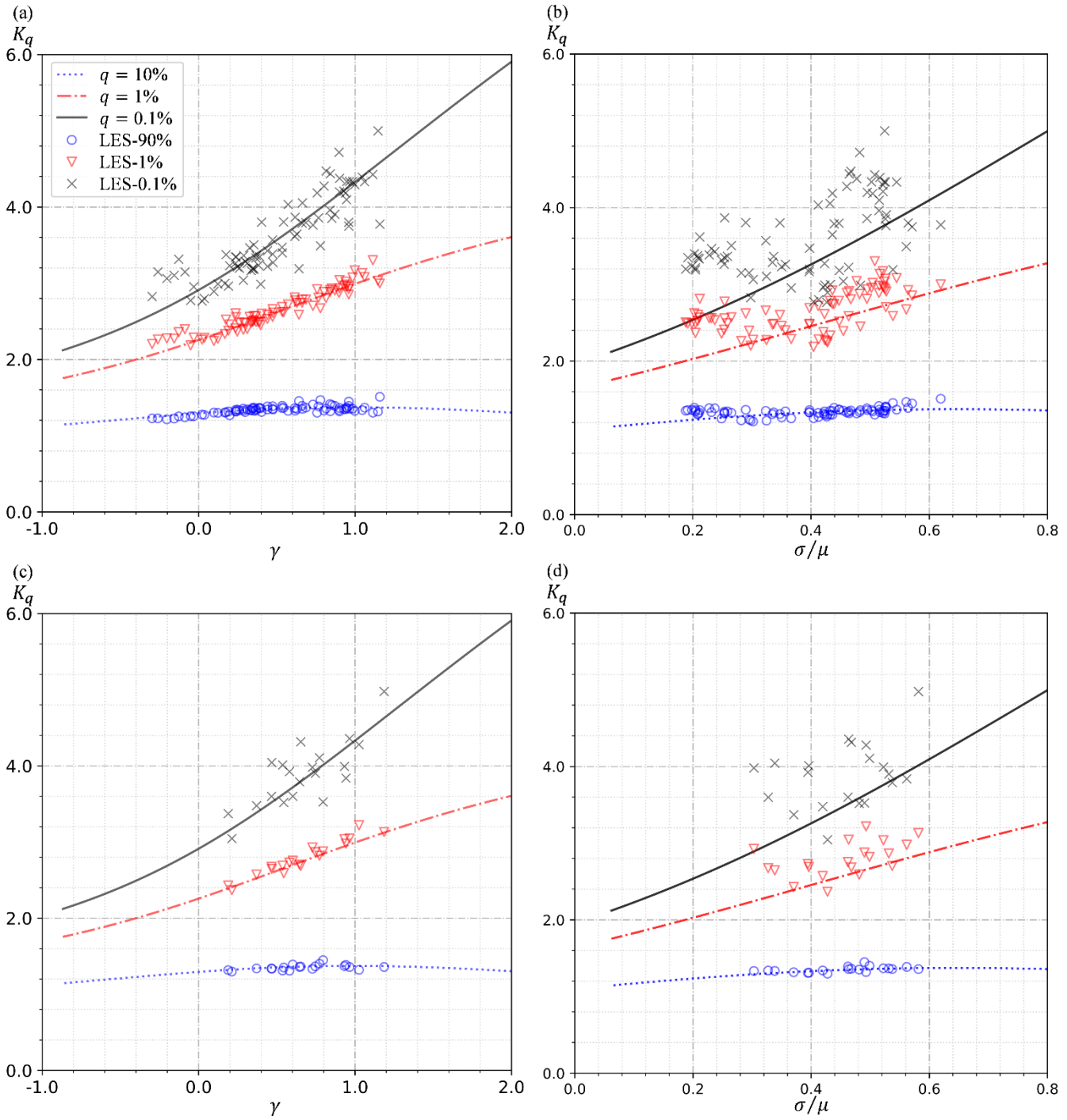

Fig. 5. Comparison of statistics and PFs K_q with q = 10%, 1% and 0.1% for (a, b) Case-IB and (c, d) Case-TPU. The x-axis in (a, c) denotes the skewness γ and in (b, d) denotes the CV σ/μ. The y-axis denotes the PF. The curves are the theoretical relationships of 3W (a, c) or 2W (b, d). The scatters are the LES results.

σ/μ (e.g., $\sigma/\mu > 0.3$), the curves of 2W are close to the LES results, while the agreements for smaller σ/μ (e.g., $\sigma/\mu < 0.3$) are worse for q = 1% and 0.1%. This is because of the relatively poor fits of 2W to the local wind field (see Wang and Okaze, 2022 for details). By comparing Fig. 5 (a) with Fig. 5 (b), it was found that the 3W method is more accurate than the 2W method for Case-IB. Fig. 5 (c, d) show the comparison of statistics with PFs for q = 10%, 1% and 0.1% of Case-TPU. Similar agreements of 3W and 2W to the LES results of Case-TPU can be found as those of Case-IB. This indicates that the 3W and 2W methods are robust for the cases with complicated building layouts. Overall, both 3W and 2W methods well predicted the PFs of Case-IB and Case-TPU, and the 3W method is more accurate than the 2W method.

In Fig. 6, the LOSWSs s_q with q = 10%, 1% and 0.1% of Case-IB calculated from the LES time-series data (x-axis) are compared with those estimated from Eq. (10) (y-axis) with the (a) 3W method and (b) 2W method. It was found that both methods have good agreements with the LES results (relative errors are within 10% at most probe points). The 3W method has better accuracy than the 2W method. Fig. 7 shows the LOSWS comparison of Case-TPU. The relative errors of the 3W method are within 10%, while those of the 2W method at several points are within 10%–20%. Overall, from the analyses of Case-IB and Case-TPU, the high accuracy and robustness of the 3W and 2W methods were confirmed.

6. Conclusion

In this study, the estimation accuracies of the low-occurrence strong wind speed at the pedestrian level by the 3W and 2W methods for an isolated building case (Case-IB) and an actual urban case (Case-TPU) were analyzed. The LES of Case-IB was from a LES database and was already validated in previous studies. The LES of Case-TPU was validated to have acceptable accuracy by comparing the effective mean wind speed and standard deviations with those of the WTE. It was found that the peak factors with exceedance probabilities q = 10%, 1% and 0.1% of the 3W and 2W methods are close to those of the LES results. The relative errors of the low-occurrence strong wind speed with q = 10%, 1% and 0.1% predicted by both methods are within 10% at most probe points for both Case-IB and Case-TPU. The high accuracy and robustness of the 3W and 2W methods for the case with complicated building layout were confirmed in this study.

Acknowledgments

This work was supported by the Japan Society for the Promotion of Science (JSPS) KAKENHI (Grant number: 21H01489) of Okaze, and the JSPS KAKENHI (Grant number: 21K18770) and FOREST program from JST (Grant number JPMJFR205O) of Ikegaya.

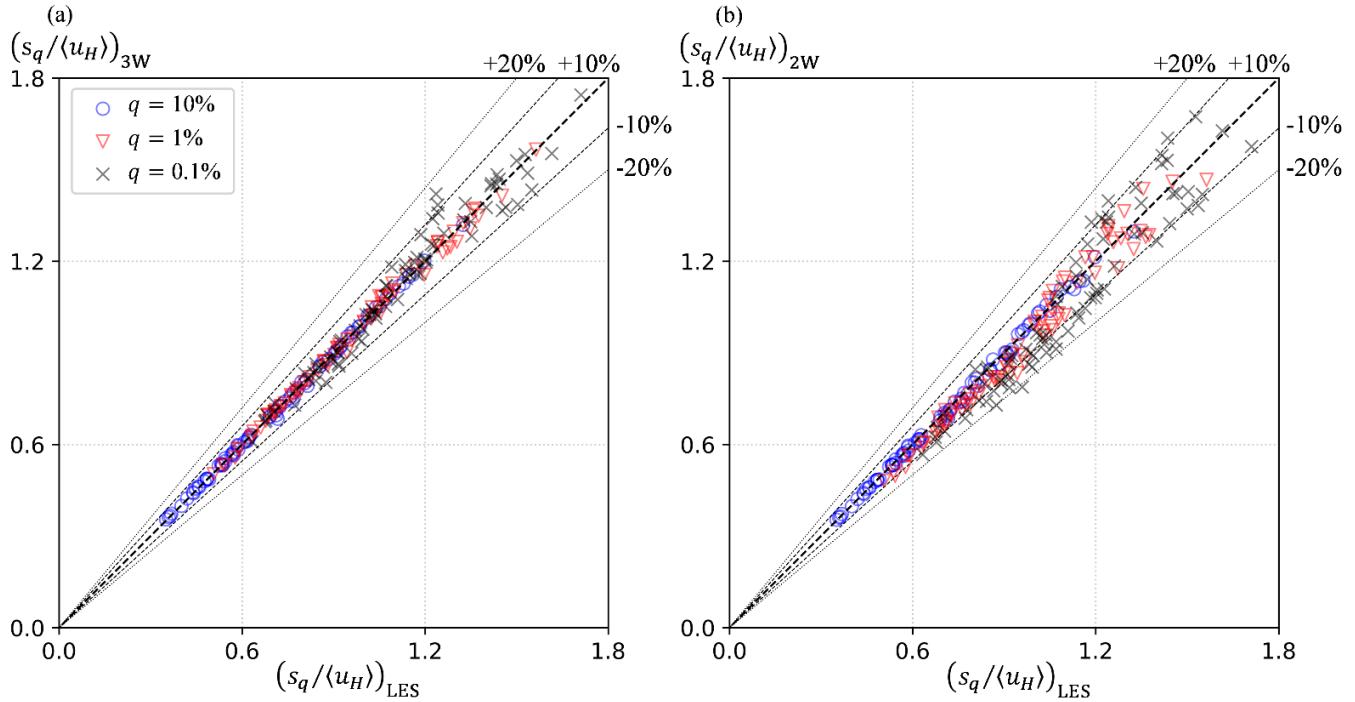

Fig. 6. Comparison of the LOSWSs with q = 10%, 1% and 0.1%. The x-axis denotes the wind speed calculated from the LES time-series data $(s_q/\langle u_H\rangle)_{LES}$ and y-axis denotes the wind speed estimated from the (a) 3W method $(s_q/\langle u_H\rangle)_{3W}$ or (b) 2W method $(s_q/\langle u_H\rangle)_{2W}$. $\langle u_H\rangle$ is the mean streamwise velocity at the building height of the inflow boundary.

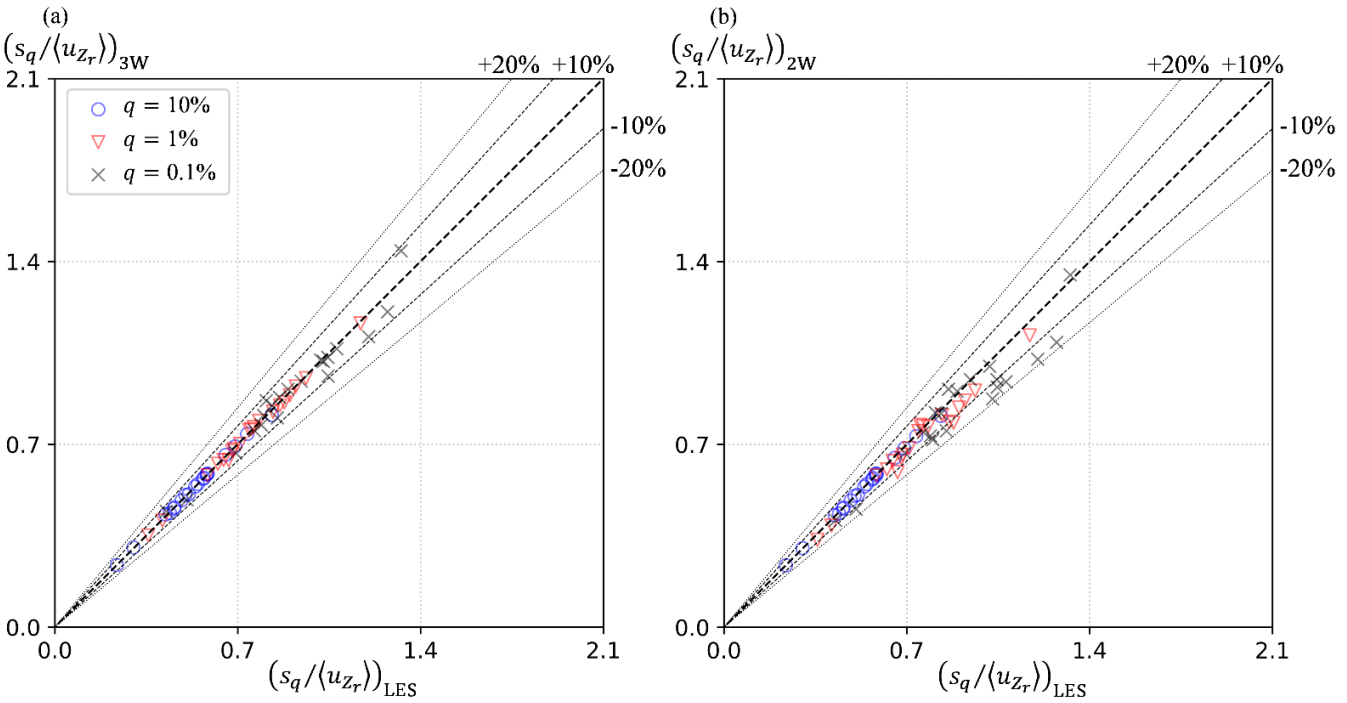

Fig. 7. Comparison of the LOSWSs with q = 10%, 1% and 0.1%. The x-axis denotes the wind speed calculated from the LES time-series data $(s_q/\langle u_{Z_r}\rangle)_{LES}$ and y-axis denotes the wind speed estimated from the (a) 3W method $(s_q/\langle u_{Z_r}\rangle)_{3W}$ or (b) 2W method $(s_q/\langle u_{Z_r}\rangle)_{2W}$.

References

AIJ benchmark Case-H. URL https://www.aij.or.jp/jpn/publish/cfdguide/index_e.htm

Blocken, B., Stathopoulos, T., van Beeck, J.P.A.J., 2016. Pedestrian-level wind conditions around buildings: Review of wind-tunnel and CFD techniques and their accuracy for wind comfort assessment. Build. Environ. https://doi.org/10.1016/j.buildenv.2016.02.004

Cao, Y., Tamura, T., Kawai, H., 2019. Investigation of wall pressures and surface fl ow patterns on a wall-mounted square cylinder using very high-resolution Cartesian mesh. J. Wind Eng. Ind. Aerodyn. 188, 1–18. https://doi.org/10.1016/j.jweia.2019.02.013

Efthimiou, G.C., Hertwig, D., Andronopoulos, S., Bartzis, J.G., Coceal, O., 2017. A Statistical Model for the Prediction of Wind-Speed Probabilities in the Atmospheric Surface Layer. Boundary-Layer Meteorol. 163, 179–201. https://doi.org/10.1007/s10546-016-0221-2

Hertwig, D., Patnaik, G., Leitl, B., 2017. LES validation of urban flow, part I: flow statistics and frequency distributions. Environ. Fluid Mech. 17, 521–550. https://doi.org/10.1007/s10652-016-9507-7

Ikegaya, N., Ikeda, Y., Hagishima, A., Tanimoto, J., 2017. Evaluation of rare velocity at a pedestrian level due to turbulence in a neutrally stable shear flow over simplified urban arrays. J. Wind Eng. Ind. Aerodyn. 171, 137–147. https://doi.org/10.1016/j.jweia.2017.10.002

Ikegaya, N., Kawaminami, T., Okaze, T., Hagishima, A., 2020. Evaluation of exceeding wind speed at a pedestrian level around a 1:1:2 isolated block model. J. Wind Eng. Ind. Aerodyn. 201, 104193. https://doi.org/10.1016/j.jweia.2020.104193

Ikegaya, N., Okaze, T., Kikumoto, H., Imano, M., Ono, H., Tominaga, Y., 2019. Effect of the numerical viscosity on reproduction of mean and turbulent flow fields in the case of a 1:1:2 single block model. J. Wind Eng. Ind. Aerodyn. 191, 279–296. https://doi.org/10.1016/j.jweia.2019.06.013

Isyumov, N., Davenport, A., 1975. The ground level wind environment in built-up areas, in: Proceedings of the 4th International Conference on Wind Effects on Buildings and Structures. pp. 403–422.

Kawaminami, T., Ikegaya, N., Hagishima, A., Tanimoto, J., 2018. Velocity and scalar concentrations with low

occurrence frequencies within urban canopy regions in a neutrally stable shear flow over simplified urban arrays. J. Wind Eng. Ind. Aerodyn. 182, 286–294. https://doi.org/10.1016/j.jweia.2018.09.024

Murakami, S., Iwasa, Y., Morikawa, Y., 1986. Study on acceptable criteria for assessing wind environment at ground level based on residents' diaries. J. Wind Eng. Ind. Aerodyn. 24. https://doi.org/10.1016/0167-6105(86)90069-3

Okaze, T., Kikumoto, H., Ono, H., Imano, M., Ikegaya, N., Hasama, T., Nakao, K., Kishida, T., Tabata, Y., Nakajima, K., Yoshie, R., Tominaga, Y., 2021. Large-eddy simulation of flow around an isolated building: A step-by-step analysis of influencing factors on turbulent statistics. Build. Environ. 202. https://doi.org/10.1016/j.buildenv.2021.108021

Okaze, T., Kikumoto, H., Ono, H., Imano, M., Ikegaya, N., Hasama, T., Nakao, K., Kishida, T., Tabata, Y., Yoshie, R., Tominaga, Y., 2017. Large-eddy simulation of flow around buildings: Validation and sensitivity analysis. 9th Asia Pacific Conf. Wind Eng. APCWE 2017 3–6.

Rinne, H., 2008. The Weibull distribution: a handbook. CRC press.

Soligo, M.J., Irwin, P.A., Williams, C.J., Schuyler, G.D., 1998. A comprehensive assessment of pedestrian comfort including thermal effects. J. Wind Eng. Ind. Aerodyn. 77–78, 753–766. https://doi.org/10.1016/S0167-6105(98)00189-5

Stathopoulos, T., 2006. Pedestrian level winds and outdoor human comfort. J. Wind Eng. Ind. Aerodyn. 94, 769–780. https://doi.org/10.1016/j.jweia.2006.06.011

Tachibana, T., Miyashita, K., Sasaki, R., Yoshie, R., Kishida, T., 2017. Comparison of wind tunnel experiment and large eddy simulation results for pollutant dispersion in Urban Area (In Japanese). Summ. Tech. Pap. Annu. Meet. Archit. Inst. Japan 919–920.

Tominaga, Y., Mochida, A., Yoshie, R., Kataoka, H., Nozu, T., Yoshikawa, M., Shirasawa, T., 2008. AIJ guidelines for practical applications of CFD to pedestrian wind environment around buildings. J. Wind Eng. Ind. Aerodyn. 96, 1749–1761. https://doi.org/10.1016/j.jweia.2008.02.058

Vita, G., Shu, Z., Jesson, M., Quinn, A., Hemida, H., Sterling, M., Baker, C., 2020. On the assessment of pedestrian distress in urban winds. J. Wind Eng. Ind. Aerodyn. 203, 104200. https://doi.org/10.1016/j.jweia.2020.104200

Wang, H.F., Zhou, Y., Chan, C.K., Lam, K.S., 2006. Effect of initial conditions on interaction between a boundary layer and a wall-mounted finite-length-cylinder wake. Phys. Fluids 18. https://doi.org/10.1063/1.2212329

Wang, W., Cao, Y., Okaze, T., 2021. Comparison of hexahedral, tetrahedral and polyhedral cells for reproducing the wind field around an isolated building by LES. Build. Environ. 195, 107717. https://doi.org/10.1016/j.buildenv.2021.107717

Wang, W., Okaze, T., 2022. Statistical analysis of low-occurrence strong wind speeds at the pedestrian level around a simplified building based on the Weibull distribution. Build. Environ. 209, 108644. https://doi.org/10.1016/j.buildenv.2021.108644

Weibull, W., 1951. A Statistical Distribution Function of Wide Applicability. J. Appl. Mech. Vol. 18, 293–297.